1856 *Inorg. Chem.* **2011**, *50*, 1856–1861
DOI: 10.1021/ic102269y

Inorganic Chemistry
Article

Low-Spin→High-Spin Relaxation Dynamics in the Highly Diluted Spin-Crossover System $[Fe_xZn_{1-x}(bbtr)_3](ClO_4)_2$

Itana Krivokapic,[†] Pradip Chakraborty,[†] Cristian Enachescu,[‡] Robert Bronisz,[§] and Andreas Hauser*,[†]

[†] *Département de Chimie Physique, Université de Genève, 30 Quai Ernest-Ansermet, CH-1211 Genève 4, Switzerland,* [‡] *Department of Physics, Alexandru Ioan Cuza University, Blvd. Carol I, nr. 11, Iasi, Romania, and* [§] *Faculty of Chemistry, University of Wrocław, F. Joliot-Curie 14, Pl-50-383 Wrocław, Poland*

Received November 11, 2010

Whereas the neat polymeric iron(II) compound $[Fe(bbtr)_3](ClO_4)_2$, bbtr = 1,4-di(1,2,3-triazol-1-yl)butane, shows a quantitative spin transition triggered by a crystallographic phase transition centered at 107 K with a 13 K wide hysteresis, the iron(II) complexes in the diluted mixed crystals $[Fe_xZn_{1-x}(bbtr)_3](ClO_4)_2$, x = 0.02 and 0.1, stay predominantly in the $^5T_2$ high-spin state down to cryogenic temperatures. However, the $^1A_1$ low-spin state can be populated as metastable state via irradiation into the spin-allowed $^5T_2 \rightarrow {}^5E$ ligand-field transition of the high-spin species in the near-infrared. The quantum efficiency of the light-induced conversion is approximately 10% at low temperatures and decreases rapidly above 160 K. The lifetime of the light-induced low-spin state decreases from 15 days at 40 K to 30 ns at 220 K, that is, by 14 orders of magnitude. In the high-temperature regime the activation energy for the low-spin→high-spin relaxation is 1840(20) cm^{-1}.

Introduction

During the past three decades, the phenomena of thermally and light induced low-spin (LS) ↔ high-spin (HS) transitions of iron(II) complexes with a variety of ligands have been extensively studied.[1−3] The thermal transition from the low-spin $^1A_1(t_{2g}{}^6)$ state as the quantum mechanical ground state to the high-spin $^5T_2(t_{2g}{}^4\,e_g{}^2)$ state is an entropy-driven molecular process, which is observed when the zero-point energy difference between the two spin states is of the order of the thermal energy. In solution,[4] the transition behavior can be described by a Boltzmann population between the vibronic manifold of the excited HS state and the vibrational levels of the LS ground state of the complexes. Corresponding transition curves, usually given by the temperature dependence of the fraction of iron complexes in the HS state, $\gamma_{HS}(T)$, are gradual and occur over a wide temperature range. This kind of transition curve is also observed in the solid state if the cooperative interactions of elastic origin[5] between the spin-crossover complexes are small.[6,7] These interactions can always be reduced by separating the spin-crossover complexes from each other by complexes containing inert metal ions, as for instance Zn, Co, or Mn, in dilute mixed crystals.[8,9] In concentrated crystalline materials, the thermal population of the HS state as a function of temperature may strongly deviate from the simple behavior of isolated molecules because of the cooperative effects resulting from the large difference in metal−ligand bond length of up to 0.2 Å between the two spin states.[10,11] Corresponding spin transition curves are often abrupt with a complete crossover within a few degrees, and they may even occur as first-order phase transitions accompanied by a hysteresis, superstructures, steps and crystallographic phase transitions, thus presenting many intriguing aspects for investigation.[12]

The 2-dimensional polymeric compound $[Fe(bbtr)_3](ClO_4)_2$ (bbtr = 1,4-di(1,2,3-triazol-1-yl)butane) shows a complete and very abrupt thermal spin transition centered at 107 K with a comparatively broad hysteresis of 13 K accompanied by a crystallographic phase transition.[13] At 10 K, the complexes

---

*To whom correspondence should be addressed. E-mail: andreas.hauser@unige.ch.

(1) Spin Crossover in Transition Metal Compounds I−III. In *Topics in Current Chemistry*; Gütlich, P.; Goodwin, H. A., Eds.; Springer-Verlag: Heidelberg - Berlin, Germany, 2004; Vols. *233*−*235*.

(2) Gütlich, P.; Hauser, A.; Spiering, H. *Angew. Chem.* **1994**, *106*, 2971. Gütlich, P.; Hauser, A.; Spiering, H. *Angew. Chem, Int. Ed. Engl.* **1994**, *33*, 2024.

(3) Gütlich, P.; Garcia, Y.; Goodwin, H. A. *Chem. Soc. Rev.* **2000**, *29*, 419.

(4) Toftlund, H. *Monatsh. Chem.* **2001**, *132*, 1269.

(5) Spiering, H.; Meissner, E.; Köppen, H.; Müller, E. W.; Gütlich, P. *Chem. Phys.* **1982**, *68*, 65.

(6) Balde, C.; Desplanches, C.; Grunert, M.; Wei, Y. L.; Gütlich, P.; Létard, J. F. *Eur. J. Inorg. Chem.* **2008**, *34*, 5382.

(7) Balde, C.; Desplanches, C.; Gütlich, P.; Freysz, E.; Létard, J. F. *Inorg. Chim. Acta* **2008**, *361*, 3529.

(8) Jung, J.; Schmitt, G.; Wiehl, L.; Hauser, A.; Knorr, K.; Spiering, H.; Gütlich, P. *Z. Phys. B: Condens. Matter* **1996**, *100*, 523.

(9) Kohlhaas, T.; Spiering, H.; Gütlich, P. *Z. Phys. B: Condens. Matter* **1997**, *102*, 455.

(10) Guionneau, P.; Marchivie, M.; Bravic, G.; Létatd, J.-F.; Chasseau, D. *Top. Curr. Chem.* **2004**, *234*, 97.

(11) Kusz, J.; Gütlich, P.; Spiering, H. *Top. Curr. Chem.* **2004**, *234*, 129.

(12) Spiering, H. *Top. Curr. Chem.* **2004**, *235*, 171.

(13) Bronisz, R. *Inorg. Chem.* **2005**, *44*, 4463.

can be quantitatively trapped in the metastable HS state by the so-called Light Induced Excited Spin State Trapping (LIESST) effect,[14] that is, by irradiation into the spin-allowed $^1A_1 \rightarrow {}^1T_1$ absorption band centered at 548 nm (18250 cm^{-1}). As for other tetrazole and triazole spin-crossover systems, subsequent irradiation at 830 nm (12050 cm^{-1}), that is, into the spin-allowed $^5T_2 \rightarrow {}^5E$ d-d band of the HS species, while keeping the sample at 10 K, results in a light-induced repopulation of the LS state (reverse-LIESST), [15] with a final steady state value of the LS fraction of around 85% because of spectral overlap of the bands of the two species at 830 nm.[16,17] In the neat iron compound, HS→LS relaxation curves recorded between 50 and 100 K following the quantitative light-induced population of the HS state show the sigmoidal behavior typical for cooperative effects.[18,19] Whereas between 50 and 85 K the relaxation rate increases as expected, a surprising decrease is observed in the vicinity of the thermal hysteresis loop, thought to be due to strong short-range interactions leading to nucleation and growth phenomena as well as to thermal fluctuations near the critical temperature.[16,20]

For systems with a HS ground state, which of course stay predominantly in the HS state at all temperatures, it is possible to populate the LS state as metastable state at cryogenic temperatures via irradiation into the $^5T_2 \rightarrow {}^5E$ band in analogy to reverse-LIESST.[14] Only very few systems are known to exhibit this phenomenon.[17,21-24] They are, however, of considerable interest because they demonstrate the principle of a true light-induced bistability[22] as also employed in the pulsed laser switching by Bonhommeau et al.[25] In particular, except for some work at cryogenic temperatures and a short communication by Krivokapic et al.[26] on the title system, no detailed investigation and discussion of the lifetime as a function of temperature of metastable LS states has been presented to date. Herein we report such a study over a wide temperature range for the diluted mixed crystal system $[Fe_xZn_{1-x}(bbtr)_3](ClO_4)_2$ with $x = 0.02$ and 0.1, in which the iron(II) complexes remain predominantly in the HS down to 10 K.

Experimental Section

High quality $[Fe_xZn_{1-x}(bbtr)_3](ClO_4)_2$ crystals, hexagonal in shape and having well developed faces, with $x = 0.02$ and 0.1 were synthesized and grown as previously described for the neat iron compound.[13] They cleave easily perpendicular to the *c*-axis, and they are colorless at room temperature and, in contrast to the neat iron compound, they stay colorless at low temperature. The thickness of the crystals used for optical spectroscopy varied between 50 and 200 μm. Because they are bad heat conductors, crystals were mounted to cover a small aperture in a copper sample holder using silver contact glue. The sample holder was placed inside a closed cycle cryostat capable of achieving temperatures down to 4 K (Janis-Sumitomo SHI-4.5) and equipped with a programmable temperature controller (Lakeshore Model 331) allowing accurate control of the temperature sweep rate. High-quality absorption spectra were recorded on a double beam spectrometer (Varian Cary 5000). For LIESST and reverse-LIESST experiments at 10 K the light of a continuous diode pumped solid-state laser at 532 nm (ILEE VA−I-N-532) and a laser diode at 830 nm (ILEE Model Z40KV1) were used, respectively. Kinetic experiments at fixed temperature were performed using three different techniques. Below 70 K, where the relaxation is slow enough, successive spectra at given time intervals were recorded on the double beam spectrometer after irradiation with the red diode or the green DPSS laser at powers of 5 mW/mm^2 for a few minutes for quantitative transformation. From 70 to 80 K, where the relaxation is still comparatively slow, a home-built system consisting of a 0.28 m monochromator (Spex 280M) equipped with a CCD camera (Jobin-Yvon CCD 3500) and a Xenon-arc lamp (Osram XBO) was used to record full absorption spectra following irradiation with the same red laser. At higher temperatures relaxation curves were recorded using either the output of a Ti-Sapphire laser (Spectra Physics Model 3900) and a mechanical shutter or the idler output of a Nd:YAG (Quantel Brillant B) pumped optical parametric oscillator (Opotek Magic Prism) both at 830 nm for excitation, and a photomultiplier with the monochromator set to 310 nm and either a photon-counting system (Stanford Research SR400) or a digital oscilloscope (Tektronix TDK2000) for detection.

Results

Thermal Spin Transition, LIESST, and Reverse LIESST. The single crystal absorption spectra of diluted $[Fe_xZn_{1-x}(bbtr)_3](ClO_4)_2$, $x = 0.02$, on cooling down from room temperature to low temperatures at 0.5 K/min, are presented in Figure 1a with the light propagation along the *c*-axis. At this concentration and given the size of the crystals used, the d-d bands corresponding to the $^1A_1 \rightarrow {}^1T_1$ transition of the LS species and the $^5T_2 \rightarrow {}^5E$ transition of the HS species,[16] observed for the neat compound in the visible and NIR part of the spectrum, respectively, are far too weak to be observed. However, there is a more intense band in the UV, which, following Loutete et al.,[27] can be assigned to a metal−ligand charge transfer (MLCT) transition, and which may serve to monitor the spin state. At room temperature this band is centered at 285 nm and it is not very intense. As temperature decreases, the absorption intensity of the MLCT band increases, the band shape changes, and the maximum gradually moves to 307 nm. The change in band shape and concomitant increase in intensity are essentially due to the population of the LS state with its more intense MLCT transition at lower energy as compared

---

(14) Decurtins, S.; Gütlich, P.; Köhler, C. P.; Spiering, H.; Hauser, A. *Chem. Phys. Lett.* **1984**, *105*, 1.

(15) Hauser, A. *Chem. Phys. Lett.* **1986**, *124*, 543.

(16) Krivokapic, I.; Enachescu, C.; Bronisz, R.; Hauser, A. *Inorg. Chim. Acta* **2008**, *361*, 3616.

(17) Hauser, A. *J. Chem. Phys.* **1991**, *94*, 2741.

(18) Hauser, A. *Chem. Phys. Lett.* **1992**, *192*, 65.

(19) Varret, F.; Boukheddaden, K.; Codjovi, E.; Enachescu, C.; Linares, J. *Top. Curr. Chem.* **2004**, *234*, 199.

(20) Krivokapic, I.; Enachescu, C.; Bronisz, R.; Hauser, A. *Chem. Phys. Lett.* **2008**, *455*, 192.

(21) Poganiuch, P.; Decurtins, S.; Gütlich, P. *J. Am. Chem. Soc.* **1990**, *112*, 3270.

(22) Hinek, R.; Spiering, H.; Gütlich, P.; Hauser, A. *Chem.—Eur. J.* **1996**, *2*, 1434.

(23) Stassen, A. F.; Roubeau, O.; Gramage, I. F.; Linares, J.; Varret, F.; Mutikainen, I.; Turpeinen, U.; Haasnoot, J. G.; Reedijk, J. *Polyhedron* **2001**, *20*, 1699.

(24) Suemura, N.; Ohama, M.; Kaizaki, S. *Chem. Commun.* **2001**, 1538.

(25) Bonhommeau, S.; Molnar, G.; Galet, A.; Zwick, A.; Real, J. A.; McGarvey, J. J.; Bousseksou, A. *Angew. Chem., Int. Ed.* **2005**, *44*, 4069.

(26) Krivokapic, I.; Chakraborty, P.; Enachescu, C.; Bronisz, R.; Hauser, A. *Angew. Chem.* **2010**, *122*, 8688. Krivokapic, I.; Chakraborty, P.; Enachescu, C.; Bronisz, R.; Hauser, A. *Angew. Chem., Int. Ed.* **2010**, *49*, 8509.

(27) Loutete-Dangui, E. D.; Varret, F.; Codjovi, E.; Dahoo, P. R.; Tokoro, H.; Ohkoshi, S.; Eypert, C.; Létard, J. F.; Coanga, J. M.; Boukheddaden, K. *Phys. Rev. B* **2007**, *75*, 184425.

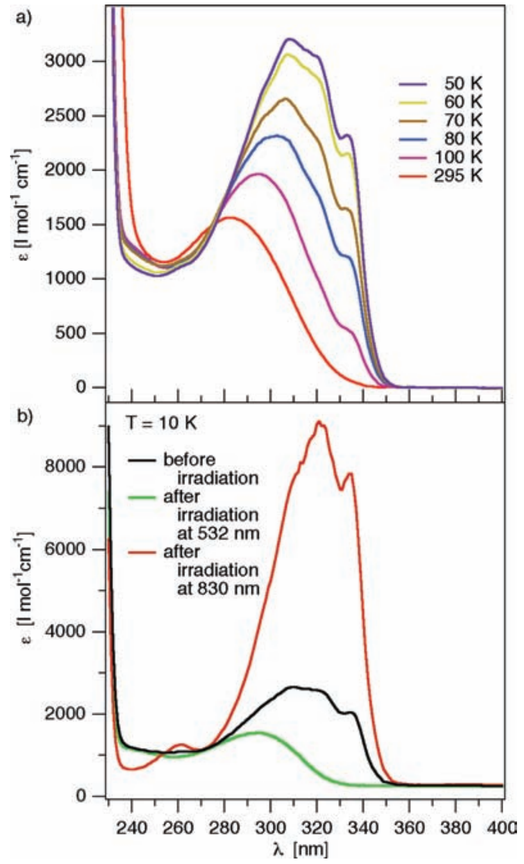

Figure 1. Single crystal absorption spectra of diluted [Fe$_x$Zn$_{1-x}$(bbtr)$_3$](ClO$_4$)$_2$, x = 0.02: (a) as function of temperature between 295 and 50 K recorded with a cooling rate of 0.5 K/min; (b) at 10 K before irradiation and following irradiation at 532 and 830 nm, respectively.

to the HS state because of the better orbital overlap resulting from the shorter metal−ligand bond length. The spectra as such do not allow for a quantitative evaluation of the transition curve, as by themselves they do not contain any information on a possible residual HS fraction at low temperature. However, by comparison with the maximum extinction coefficient in the absorption spectrum of the related neat compound [Fe(NH$_2$-trz)$_3$]Br$_2$ (NH$_2$-trz = 2-amino-triazole) estimated from ellipsometric measurements on this band by Loutete et al.[27] of the order of 10000 M^{-1} cm^{-1}, this fraction is far from negligible. As at the low iron concentration used in our mixed crystals Mössbauer spectroscopy and magnetic susceptibility measurements are not feasible, irradiation experiment according to the scheme in Figure 2 were performed at 10 K to quantify the residual HS fraction. As shown in Figure 1b, irradiation at 532 nm, that is, into the $^1A_1 \rightarrow {}^1T_1$ band known to be at this wavelength from spectra recorded on the neat compound,[16] results in a decrease of the MLCT intensity and a blue-shift compatible with a quantitative light-induced population of the HS state. On the other hand, the spectrum after irradiation at 830 nm, that is, into the $^5T_2 \rightarrow {}^5E$ band, like-wise known to be at this wavelength from spectra on the neat compound[16] is 4 times more intense than the one before irradiation. Thus, irradiation into the weak absorption band of the HS species results in a much higher population of the LS state than observed by just cooling the sample. In analogy to the neat compound, we assume that the maximum LS fraction, γ_{LS}, that can be obtained with irradiation at 830 nm is around 85%.[16] This, in turn allows an estimate of the residual HS fraction at 10 K of 0.78%. Figure 3 shows the spin transition curve, plotted as the HS fraction γ_{HS} versus T, thus obtained for diluted [Fe$_x$Zn$_{1-x}$(bbtr)$_3$](ClO$_4$)$_2$, x = 0.02, recorded with the sweeping rate of 0.2 K/min for the temperature range 295 to 100 K and of 0.1 K/min from 100 to 10 K. It can be concluded that for the diluted system, the zero-point energy difference between the two spin states is very small or almost zero. The observed residual HS fraction below 60 K can be due to several reasons: (a) an inhomogeneous distribution of the zero-point energy difference with a large fraction of the complexes having the HS state as quantum mechanical ground state; or (b) the LS ⇆ HS relaxation becoming so slow that even with a temperature scan rate of 0.1 K/min the HS state is thermally trapped; and (c) a true

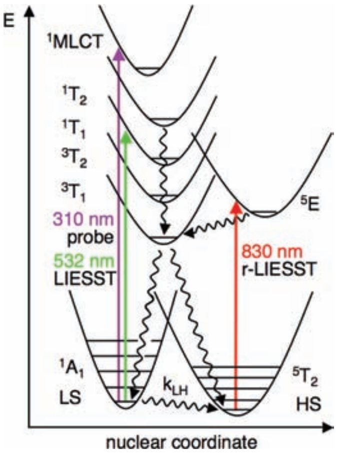

Figure 2. Schematic representation of the ligand-field and MLCT states of an octahedral iron(II) HS complex close to the spin-crossover point. Arrows indicate pathways for LIESST and reverse-LIESST upon irradiation into ligand-field states. In dilute systems, where the ligand-field transitions are too weak, MLCT transitions may be used to monitor the spin state. In the title compound, the latter is at comparatively high energy and well separated from the ligand-field transitions.

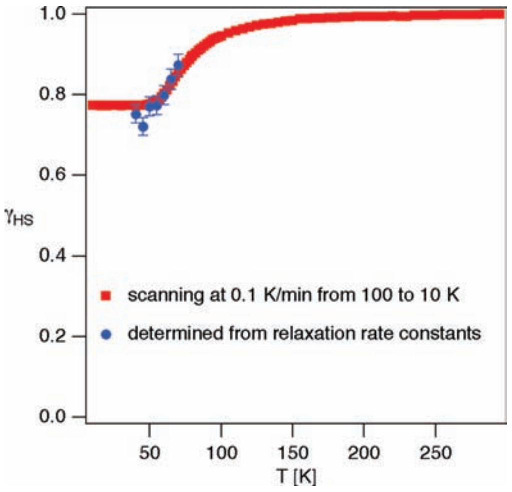

Figure 3. Spin transition curve of diluted [Fe$_x$Zn$_{1-x}$(bbtr)$_3$](ClO$_4$)$_2$, x = 0.02, (solid red squares) with a constant cooling rate of 0.2 K/min from 295 to 100 and 0.1 K/min from 100 to 10 K, (solid blue circles) derived from full or partial relaxation curves as described in the text.

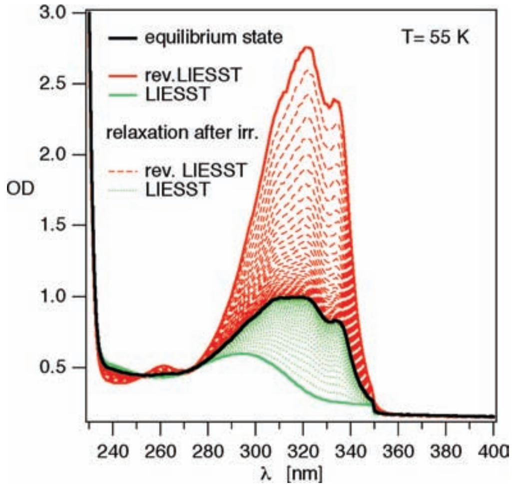

Figure 4. Evolution of the absorption spectrum after irradiation at 532 and at 830 nm, respectively recorded at time intervals of 10 min, $T = 55.0$ K. (solid red lines) spectrum right after irradiation at 830 nm, (solid black lines) equilibrium spectrum at 55 K and last spectrum after full relaxation, (solid green lines) spectrum right after irradiation at 532 nm, evolution of the spectra during the relaxation after irradiation at 830 nm (dashed red lines) and at 532 nm (dotted green lines).

residual HS fraction at thermal equilibrium. In the highly diluted system elastic interactions between spin-crossover complexes can be ruled out as possible reason. Before further discussing the thermal spin transition, it is necessary to look at the relaxation in some detail.

LS→HS Relaxation. As described above, the diluted system [Fe$_x$Zn$_{1-x}$(bbtr)$_3$](ClO$_4$)$_2$ shows both LIESST and reverse-LIESST at low temperatures, and below 50 K the relaxation to the thermodynamically stable state is very slow. Figure 4 shows the evolution of the absorption spectrum at 55 K upon irradiation at 532 nm (100% light-induced population of the HS state) and at 830 nm (85% light-induced population of the LS state in the steady state). Both sets of spectra converge to the same final spectrum corresponding to a HS fraction of 77.5%, which is only very little lower than the value obtained from the temperature scan experiment.

Analogous experiments were performed between 40 and 70 K, that is, in a temperature range, where relaxation processes are slow and the HS fraction can be easily followed quantitatively by taking full spectra. The corresponding relaxation curves, plotted as $\gamma_{\rm LS}(t)$, for both the HS→LS and the LS→HS relaxation are shown in Figure 5. Figure 5b shows the curves at 45 and 55 K on an expanded time scale. As often found for dilute systems, they are all perfectly single exponential. This indicates that the inhomogeneous distribution of the zero-point energy is negligible. For a quantitative evaluation of the relaxation curves, simultaneous fits on both curves at a given temperature were performed, with the function

$$\gamma_{\rm LS}(t) = (\gamma_{\rm LS}^0 - \gamma_{\rm LS}^\infty){\rm e}^{-k_{\rm obs}t} + \gamma_{\rm LS}^\infty \qquad (1)$$

where $\gamma_{\rm LS}^\infty$ is the LS fraction at equilibrium and $\gamma_{\rm LS}^0$ the initial LS fraction after irradiation, that is, 0.85 for the LS→HS relaxation and 0 for the HS→LS relaxation. The observed rate constant is given by

$$k_{\rm obs} = k_{\rm HL} + k_{\rm LH} \qquad (2)$$

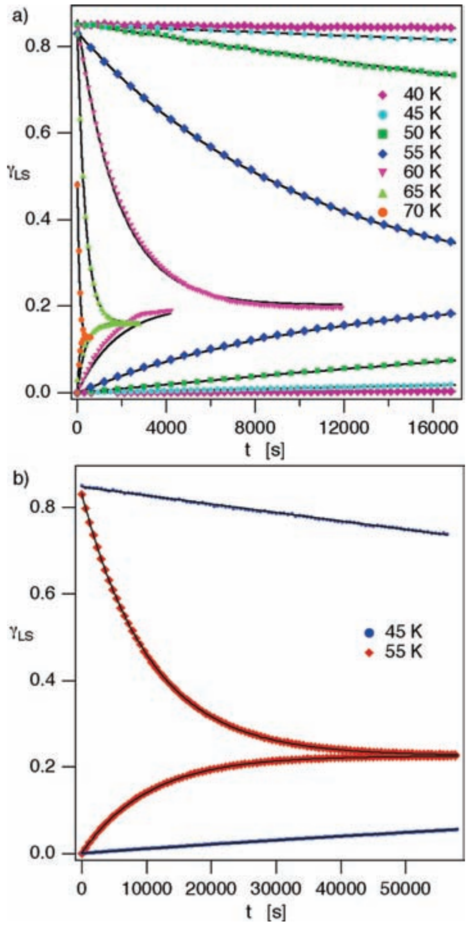

Figure 5. HS→LS and the LS→HS relaxation curves determined from full absorption spectra after irradiation at 532 and 830 nm, respectively: (a) between 40 to 70 K; (b) at 45 and 55 K on an expanded time scale; full lines: global exponential fits as described in the text.

and the equilibrium constant by

$$K = \frac{\gamma_{\rm HS}^\infty}{\gamma_{\rm LS}^\infty} = \frac{k_{\rm LH}}{k_{\rm HL}} \qquad (3)$$

with $\gamma_{\rm HS} + \gamma_{\rm LS} = 1$ at all times. Thus, from the relaxation curves $k_{\rm HL}$, $k_{\rm LH}$ and $\gamma_{\rm LS}^\infty$ as well as $\gamma_{\rm HS}^\infty$ can be determined accurately via a global least-squares fit, even for the partial curves at 40, 45, and 50 K where it would take too long to record full curves. At the lowest temperature, that is, at 40 K for instance, $k_{\rm obs} = 7.4(3) \times 10^{-7}$ s^{-1} ($\tau = 15$ days), with values for $k_{\rm LH}$, $k_{\rm HL}$ and $\gamma_{\rm HS}^\infty$ of $5.6(2) \times 10^{-7}$ s^{-1}, $1.8(1) \times 10^{-7}$ s^{-1}, and 0.75(2), respectively. The values thus obtained for $\gamma_{\rm HS}^\infty$ for this and other temperatures are included in Figure 3. They clearly show that in the temperature scan experiment with a cooling rate of 0.1 K/min below 100 K, the HS state is only marginally trapped below 50 K, and the residual HS fraction therefore corresponds to a thermodynamic equilibrium. The corresponding rate constants, that is, both $k_{\rm LH}$ and $k_{\rm HL}$, are shown in Figure 6.

At higher temperatures it is no longer possible to record full relaxation curves starting from a well-defined value of the light-induced LS fraction. For the single exponential process in question this is not important. Despite the small quantum efficiency of the light-induced population of the LS state and the low value of the extinction

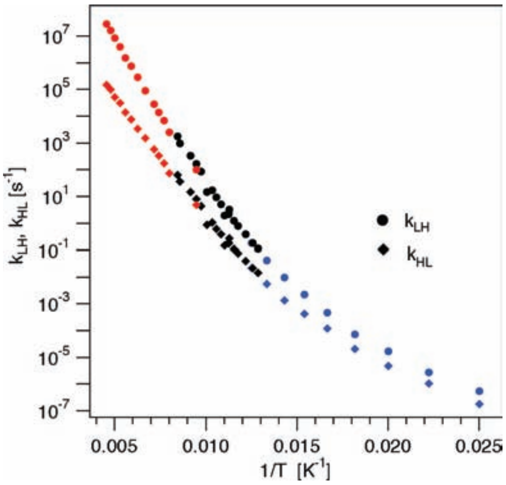

Figure 6. Relaxation rate constants, k_{LH} and k_{HL} plotted on a logarithmic scale versus $1/T$ from 40 to 220 K following the different protocols as described in the Experimental Section: (solid blue circles, solid blue diamonds) determined from full spectra recorded with a dual beam spectrometer or a CCD system, respectively, at given time intervals following CW excitation, (solid black circles, solid black diamonds) recorded at a fixed wavelength of 310 nm using a PM and pulsed excitation from chopped Ti-Sapphire CW laser or (solid red circles, solid red diamonds) a ns pulsed laser at 830 nm.

coefficient of only 4 M^{-1} cm^{-1} at the pump wavelength, the LS→HS relaxation can be easily monitored at the wavelength of the very intense ^{1}MLCT transition of the LS species according to the scheme of Figure 2. Indeed, an initial light-induced population of the LS state of only around 2% is necessary to determine the rate constant of the single exponential relaxation decay precisely. In the Supporting Information, relaxation curves between 80 and 220 K recorded according to the different protocols described in the Experimental Section can be found. The corresponding relaxation rate constants, k_{LH} and k_{HL} calculated from k_{obs} and γ_{HS} as a function of temperature are included in Figure 6. To enhance the signal at higher temperatures a somewhat more heavily doped crystal with $x = 10\%$ rather than the standard 2% sample was used. The high-temperature limit is given by the relaxation time, which decreases from about 15 days at 40 K to 33 ns, that is, to the limit of the setup, at 220 K. At the same time the amplitude of the transient signal decreases rapidly with increasing temperature above 160 K, indicating that the quantum efficiency of the light-induced population of the low-spin state decreases at higher temperature.

Discussion

Whereas in the neat iron compound the thermal spin transition is very abrupt and complete, in the dilute system studied here it is gradual and far from complete. The former is expected as in dilute systems, and thus in the absence of cooperative effects, spin transitions are in general gradual. Whereas at room temperature the population of the HS spin state is close to unity, there is a considerable residual HS fraction at low temperatures. Is this due to thermal trapping even at a cooling rate as low as 0.1 K/min because of the very slow relaxation below 50 K, or does it correspond to a true thermodynamic equilibrium? That there is some trapping is clear by comparison with the HS fraction below 50 K as determined from the extrapolation of the relaxation experiments to $t \rightarrow \infty$, which show a somewhat lower HS fraction of 0.74(2) as compared to 0.78 from the temperature scan experiment. The former corresponds to the real thermodynamic equilibrium even below 50 K. What then is the reason for this rather large residual HS fraction at low temperature? As mentioned above, it could, as is often the case in amorphous media and badly crystallized systems, be due to an inhomogeneous distribution of the zero-point energy difference in the mixed crystals. However, this can be ruled out on the basis of the relaxation curves, which all show perfectly single exponential behavior, indicating a very well-defined value of the rate constant and thus a well-defined zero-point energy difference between the two states. The residual HS fraction must therefore be due to the fact that in the high-symmetry system under study, the trigonal component of the ligand-field and spin–orbit coupling split the $^5T_2$ multiplet in such a way that one nondegenerate component of the HS electronic multiplet is the overall quantum mechanical ground state, but that the LS state is almost isoenergetic with it. Thus the residual HS fraction at low temperature is given by the low-temperature vibrational entropy difference due to low-frequency vibrations only.[28,29]

To date the vast majority of relaxation studies on spin-crossover and related systems have been performed for the HS→LS relaxation following excitation into either dd or MLCT bands of the LS species. This is facilitated by the larger extinction coefficients of the LS absorption bands and the almost unity quantum efficiency of the light-induced LS→HS conversion. The reverse process is considerably more difficult to study because of the comparatively weak absorption of the only band of the HS species, namely, the $^5T_2 \rightarrow {}^5E$ transition, well separated from LS bands and the much lower quantum efficiency of the light-induced HS→LS conversion. Thus, only a few studies looked at the reverse process,[21,22] and none of them were performed over the large temperature range reported here. At higher temperatures the LS→HS relaxation proceeds via quasi-classical thermal activation. A linear fit of ln[k_{LH}] versus $1/T$ for temperatures above 100 K gives an activation energy $E_a = 1840(20)$ cm^{-1} and a frequency factor $A = 7.3(5) \times 10^{12}$ s^{-1}. Both the frequency factor and the activation energy are considerably larger than what has been reported for the more common case of the HS→LS relaxation both in solution[30] as well as in the solid state.[31,32] The activation energy and the frequency factor are both directly correlated to the zero-point energy difference between the two states. In fact they both decrease with increasing zero-point energy difference.[33] Spin-crossover systems for which the HS→LS relaxation via LIESST can be measured to higher temperatures, that is, well into the activated region, must have comparatively high thermal transition temperatures. For these, the zero-point energy difference between the two states and therefore the driving force for the HS→LS relaxation is quite large, and as a result, the activation energy and the frequency factor are

---

(28) Tuchagues, J.-P.; Bousseksou, A.; Molnar, G.; McGarvey, J. J.; Varret, F. *Top. Curr. Chem.* **2004**, *235*, 85.

(29) Bousseksou, A.; Verelst, M.; Constant-Machado, H.; Lemercier, G.; Tuchagues, J.-P.; Varret, F. *Inorg. Chem.* **1996**, *35*, 100.

(30) Beattie, J. K. *Adv. Inorg. Chem.* **1988**, *32*, 1.

(31) Hauser, A. *Top. Curr. Chem.* **2004**, *234*, 155.

(32) Létard, J.-F.; Chastanet, G.; Nguyen, O.; Marcen, S.; Marchivie, M.; Guionneau, P.; Chasseau, D.; Gütlich, P. *Monatsh. Chem.* **2003**, *134*, 165.

(33) Hauser, A. *Comments Inorg. Chem.* **1995**, *17*, 17.

comparatively small. For the reverse process, namely, the determination of the LS→HS relaxation via reverse LIESST to higher temperatures, there is no such restriction. In the present case, the two states are quasi isoenergetic, resulting in the highest possible activation energy. Nevertheless, the value of the activation energy is still somewhat below the classical height of the barrier estimated on the basis of the characteristic metal–ligand bond length difference of 0.2 Å between the two states.[33] However, it approaches the high temperature limit as predicted for a non-adiabatic multiphonon process[34] in the limit of a very small zero-point energy difference.[33] Likewise, it is evident that below 100 K there are substantial deviations from classical thermally activated behavior. According to Buhks et al.,[34] these deviations with the relaxation rate constant going toward a limiting value at $T \rightarrow 0$ are characteristic for nuclear tunnelling. It is interesting to note that the low-temperature tunnelling rate constant for the LS→HS relaxation in the present system is almost identical to the one of the HS→LS relaxation in the dilute spin-crossover system $[Fe_xZn_{1-x}(ptz)_6](BF_4)_2$, ptz = 1-propyltetrazole,[35] which likewise has a very small zero-point energy difference but with the LS state as quantum mechanical ground state, and which is structurally related to the title compound.

Conclusions

There are a number of systems where LIESST and reverse-LIESST have been observed on the same system and where it has been possible to successfully and repeatedly create the corresponding metastable states, and in some cases even to obtain a light-induced bistability[22] and hysteresis behavior.[36−38] Indeed bistability with respect to external stimuli in conjunction with optical and magnetic properties of spin-crossover materials constitutes an interesting and essential aspect for practical application as optical switches and in magneto-optical storage devices. It gives us the possibility to address the spin states exclusively through light irradiation. Likewise the reversibility of the process is a desirable property for memory devices. Another requirement is that these materials should be functional at room temperature. Whereas a number of studies have shown the possibility of LS→HS switching using pulsed laser irradiation inside the thermal hysteresis in highly cooperative systems,[38] the conditions under which the reverse process can be achieved are not clear as yet. The detailed investigation of reverse-LIESST and the LS→HS relaxation in diluted $[Fe_xZn_{1-x}(bbtr)_3](ClO_4)_2$, x = 2%, will thus help to design highly cooperative systems for efficient optical bidirectional switching at higher temperatures in the future. In the present system, the lifetime of the light-induced low-spin state decreases from 15 days at 40 K to 33 ns at 220 K. The corresponding variation of the relaxation rate constant of a single process of 14 orders of magnitude between 40 and 220 K determined experimentally is unique. It is due to the close to zero zero-point energy difference and the large bond length difference between the two states, resulting in a maximum value of the classical energy barrier of 1840(20) cm^{-1} and a minimum value for the low-temperature tunnelling rate. The single process can be followed over such a large temperature range and over so many orders of magnitude because there are no competing relaxation processes. In view of the strong cooperative effects in the pure iron compound, which stabilize the LS state at low temperatures, it will be interesting to study the light-induced spin transition and the relaxation behavior in a mixed crystal series also at higher iron concentrations, which offer the possibility to fine-tune the value of the zero-point energy difference around zero via cooperative effects.

Acknowledgment. This work was supported by the Swiss National Science Foundation (Grant 200020-125175), the NoE of the EU "MAGMANet" (Grant No UE6-NMP3-CT05-515767), the Romanian CNCSIS-UEFISCSU (Project No PNII-Idei 9/2010) and the Ministry of Science and Higher Education of Poland (Grant 2493/B/H03/2008/34).

Supporting Information Available: Further details are given in Figures S1−S3. This material is available free of charge via the Internet at http://pubs.acs.org.

---

(34) Buhks, E.; Navon, G.; Bixon, M.; Jortner, J. *J. Am. Chem. Soc.* **1980**, *102*, 2918.

(35) Jeftic, J.; Hauser, A. *J. Phys. Chem. B* **1997**, *101*, 10262.

(36) Létard, J. F.; Capes, L.; Chastanet, G.; Moliner, N.; Létard, S.; Real, J. A.; Kahn, O. *Chem. Phys. Lett.* **1999**, *313*, 115.

(37) Enachescu, C.; Varret, F.; Codjovi, E.; Linares, J.; Floquet, S.; Manikandan, P.; Manoharan, P. T. *J. Phys. Chem. B* **2006**, *110*, 5883.

(38) Cobo, S.; Ostrovskii, D.; Bonhommeau, S.; Vendier, L.; Molnar, G.; Salmon, L.; Tanaka, K.; Bousseksou, A. *J. Am. Chem. Soc.* **2008**, *130*, 9019.